PHYSICAL REVIEW B **80**, 100405(R) (2009)

Nucleation of a vortex-antivortex pair in the presence of an immobile magnetic vortex

Volodymyr P. Kravchuk,[1,*] Yuri Gaididei,[1] and Denis D. Sheka[2]
[1]*Bogolyubov Institute for Theoretical Physics, 03143 Kiev, Ukraine*
[2]*National Taras Shevchenko University of Kiev, 03127 Kiev, Ukraine*
(Received 2 March 2009; published 18 September 2009)

It is shown that under the action of a rotating magnetic field an *immobile* vortex, contrary to general belief, can nucleate a vortex-antivortex pair and switch its polarity. Two different kinds of OOMMF micromagnetic modeling are used: (i) the original vortex is pinned by the highly anisotropic easy-axis impurity at the disk center and (ii) the vortex is pinned by artificially fixing the magnetization inside the vortex core in the planar vortex distribution. In both types of simulations a dip creation with a consequent vortex-antivortex pair nucleation is observed. Polarity switching occurs in the former case only. Our analytical approach is based on the transformation to the rotating frame of reference, both in the real space and in the magnetization space, and on the observation that the physical reason for the dip creation is softening of the dipole magnon mode due to magnetic field rotation.

DOI: 10.1103/PhysRevB.80.100405 PACS number(s): 75.75.+a, 75.10.Hk

A magnetic vortex forms a ground state of submicron sized magnetic particles, which provides high density storage and high speed magnetic RAM.[1] One bit of information corresponds to the upward or downward magnetization of the vortex core (vortex polarity). Exciting the vortex motion by high-frequency magnetic fields or by a spin polarized current, one can switch the vortex polarity on a picosecond time scale. It is known that the switching process is mediated by a vortex-antivortex pair creation.[2] Typically to observe this switching phenomenon, one has to excite the low frequency gyroscopic mode, which causes the vortex gyromotion. The vortex-core switching was observed experimentally and by simulations only for a moving vortex. Moreover, there is a strong belief that the switching occurs "whenever the velocity of vortex-core motion reaches its critical velocity" v_{cri},[3] which is determined only by the exchange constant A; for typical soft materials it is about $v_{\mathrm{cri}} \sim 300$ m/s.[3,4]

In this Rapid Communication we predict the switching for the *immobile* vortex by a rotating magnetic field. The switching picture also involves the mechanism of a dip formation followed by a nucleation of vortex-antivortex pair. We found that the driving force for the dip formation is the in-plane magnetization inhomogeneity, created by a vortex together with the rotating magnetic field; the vortex out-of-plane structure and the vortex velocity are not principle for this mechanism. These conclusions are confirmed by the micromagnetic simulations and by a simple analytical picture.

Recently, we have reported about the vortex-core switching by the homogeneous rotating field $\boldsymbol{B}(t)=(B\cos\omega t, B\sin\omega t, 0)$ in the 10 GHz range,[5] which is much higher than the gyrofrequency and is in the frequency range of the higher azimuthal mode with $|m|=1$.[6–8] Opposite to the pumping with the low gyrofrequency, which results in the visible gyroscopic motion of the vortex position, the high-frequency field leads to small amplitude (few nm) oscillations of the vortex position, see the trajectories in Fig. 3 of Ref. 5. Therefore the question appears: is it necessary for the vortex to move at all in order to switch its polarity?

To achieve switching of the immobile vortex we have numerically performed two different kinds of modeling using OOMMF micromagnetic simulations:[9] (i) we have pinned the vortex by the highly anisotropic easy-axes impurity at the disk center (see Fig. 1). Since the magnetization is always held perpendicular to the disk plane within the impurity, shifting of the vortex core from the impurity leads to an increase of magnetostatic energy of the system. Therefore one can use such type of impurity to pin the vortex with out-of-plane core structure in conditions of a weak external influence. Initially, the vortex has a positive polarity $p=+1$. By applying the ac field, which rotates against the vortex polarity, $\omega p<0$ [in a clockwise (CW) direction from a reader's point of view], one can observe the formation of the dip (the localized region with appreciable out-of-plane magnetization m_z) near the pinned vortex [see Fig. 1(a)]. Under the action of the field the dip deepens [see Fig. 1(b)]. When the amplitude of the dip reaches its maximum value, a vortex–antivortex pair is created [see Fig. 1(c)]. The positions of the vortices and the antivortex can be identified by the cross section of isosurfaces $m_x=0$ and $m_y=0$.[10] One can identify from Fig. 1(c) positions of newborn vortex and antivortex as well as the position of the initial vortex, which is still at origin, as it is seen from the figure. The further dynamics is well known:[2,10–12] the newborn antivortex annihilates with pinned original vortex, and eventually only the newborn vortex with the opposite polarity survives [see Fig. 1(d)].

In order to achieve the immobility of the vortex the diameter of the impurity has to be comparable with the vortex-core size, which is of the same order of magnitude as the amplitude of the vortex oscillations under considered high-frequency field.[5] To avoid possible ambiguities we also used an artificial manner of the vortex pinning: (ii) we programmatically pinned the vortex core by setting the magnetization of the four central mesh cells in the planar vortex distribution,[13] where the normalized magnetization $\boldsymbol{m}=(\sqrt{1-m_z^2}\cos\phi, \sqrt{1-m_z^2}\sin\phi, m_z)$ takes a form $m_z=0$ and $\phi=\chi+\mathfrak{C}\pi/2$ with (r,χ) being the polar coordinates in the disk plane and $\mathfrak{C}=\pm 1$ being the vortex chirality. By this artificially pinned vortex state configuration, the central vortex is *a priori* immobile, and moreover, without out-of-plane structure. The direction of the dip magnetization is determined only by the direction of the field rotation: if we apply

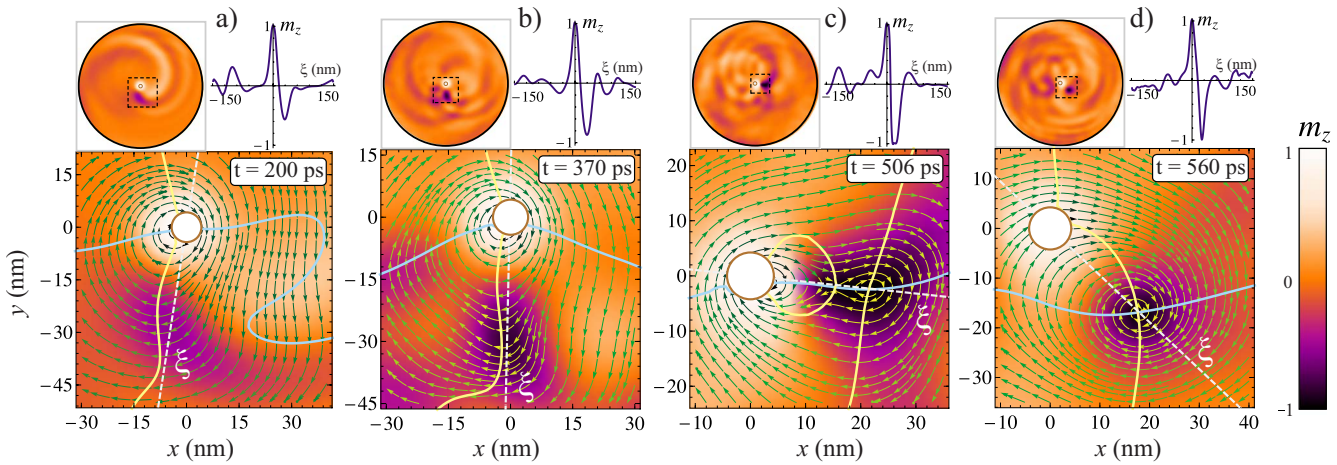

FIG. 1. (Color online) The modeling of the vortex-antivortex pair formation for the pinned vortex on the impurity in the Py disk (300 nm diameter, 20 nm thickness, and 9 nm is a diameter of impurity with the easy-axis anisotropy $K=17$ MJ/m^3). Snapshots describe the magnetization dynamics at different times under the influence of the rotating in-plane magnetic field ($\omega=6$ GHz, $B=20$ mT). The lower row shows the in-plane magnetization dynamics near the disk center. The in-plane magnetization distribution is indicated by streamlines with arrows. Blue and yellow solid lines correspond to the isosurfaces $m_x=0$ and $m_y=0$, respectively. The out-of-plane magnetization profiles along the line ξ crossing the impurity is shown above the snapshots (right pictures). Left pictures indicate the in-plane magnetization dynamics in the whole disk.

a CCW (CW) field, there appears a dip with $m_z>0$ ($m_z<0$) (see Fig. 2). This high-frequency field also excites the magnon modes. One can resolve the mode with $m=1$ in Figs. 2(a) and 2(c), and the mode with $m=2$ in Fig. 2(b). During the pumping, the amplitude of the dip increases, and finally, the vortex-antivortex pair is created [see Fig. 2(d)]. Note that the newborn antivortex cannot annihilate with the initial vortex in the fixed core model: it either annihilates with the newborn vortex and the scenario repeats itself again and again, or it stays near the original fixed vortex, while the newborn vortex is dragged by the field.

The goal of our study is to reveal the mechanism of the dip formation. We follow the simplest model of fixed core planar vortex. Numerically, we found that the dip formation occurs in a well defined range of the field parameters (ω,B) (see Fig. 3). When the frequency of the field is less than a critical value ω_{c_1}, the dip is not formed. The same happens for the high-frequency field ($\omega>\omega_{c_2}$). More accurately, out of the borders of the range $(\omega_{c_1},\omega_{c_2})$, the depth of the dip rapidly decreases, as indicated by color coding in Fig. 3. Both critical values ω_{c_1} and ω_{c_2} depend on the disk thickness, which points to the nonlocal magnetostatic nature of this phenomenon. An example of the temporal dependence of the dip depth is plotted in Fig. 4 for a certain disk thickness (15 nm) for which $\omega_{c_1}=8$ GHz and $\omega_{c_2}=12$ GHz. For $\omega<\omega_{c_1}$ just as for $\omega>\omega_{c_2}$ the dip depth does not reach its minimal value $m_z=-1$, unlike the case $\omega_{c_1}<\omega<\omega_{c_2}$, when the vortex-antivortex pair is born. The depth of the dip usually makes a number of oscillations while it reaches the limit value. Only for frequencies which are close to the eigenfrequency of the mode with $|m|=1$, it changes monotonously.

The magnetic energy of the system under consideration

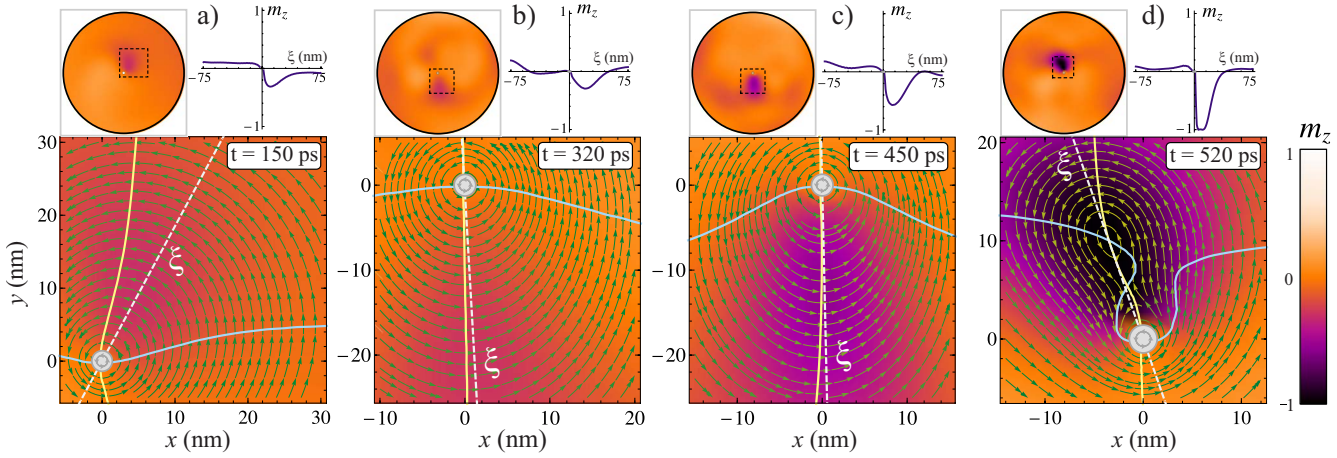

FIG. 2. (Color online) The vortex-anivortex pair formation in a Py disk (150 nm diameter and 20 nm thickness) within the fixed core modeling (see the details in the text) under the CW field influence ($\omega=8$ GHz, $B=20$ mT). Gray disk denotes the region of the artificially fixed spins. Other notations are the same as in Fig. 1.

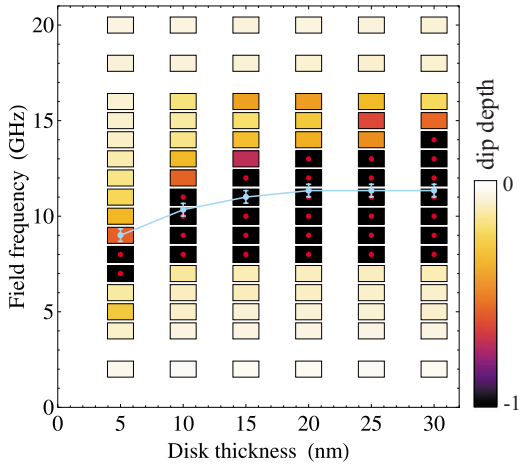

FIG. 3. (Color online) Diagram of the frequency range, where the dip formation occurs for a fixed diameter disk ($2R=150$ nm) under the influence of a fixed field amplitude ($B=20$ mT) rotating field. Colors indicate the depth of the dip. The circle over black symbol indicates that the vortex-antivortex pair creation occurs. Light blue (gray) symbols indicate frequencies of the azimuthal eigenmode with $m=1$.

consists of three terms: $\mathcal{E}=\int d\boldsymbol{r}(W_{\rm ex}+W_{\rm ms}+W_{\rm f})$, where $W_{\rm ex}=\ell^2(\nabla \boldsymbol{m})^2$ is the exchange energy density, $W_{\rm ms}=\frac{1}{8\pi}\int d\boldsymbol{r}'(\boldsymbol{m}(\boldsymbol{r})\cdot\nabla)(\boldsymbol{m}(\boldsymbol{r}')\cdot\nabla')|\boldsymbol{r}-\boldsymbol{r}'|^{-1}$ is the density of magnetostatic interaction energy, and $W_{\rm f}=-b\sqrt{1-m_z^2}\cos(\phi-\omega t)$ is the interaction with a magnetic field $\boldsymbol{b}=(b\cos\omega t, b\sin\omega t, 0)$. Here and below normalized quantities are used: $\mathcal{E}=E/(4\pi M_s^2)$, $b=B/(4\pi M_s)$, ω and t are measured in units Ω and $1/\Omega$, respectively, where $\Omega=4\pi\gamma M_s$ and γ is the gyromagnetic ratio. In the no-driving case $b=0$ the magnetic energy $\mathcal{E}$ of *cylindrical* nanoparticles is invariant under transition into a rotated frame of reference: $\tilde{\chi}=\chi-\alpha$, $\tilde{\phi}(\tilde{\chi})=\phi(\chi)-\alpha$. This means that the quantity $J=M_z+L_z$ with $M_z=\int d\boldsymbol{r}(1-m_z)$ being the renormalized magnetization along the cylindrical axis z and $L_z=-\int d\boldsymbol{r}(1-m_z)\partial_\chi\phi$ being the z-component of the orbital momentum, is conserved. This fact suggests that in the presence of the rotating magnetic field it is convenient to transfer into rotating frame of reference $\tilde{\chi}=\chi-\omega t$, $\tilde{r}=r$, $\tilde{t}=t$, $\tilde{\phi}(\tilde{\chi})=\phi(\chi=\tilde{\chi}+\omega t)-\omega\tilde{t}$, where the total energy is time independent and has the form $\tilde{\mathcal{E}}=\mathcal{E}-\omega J$, where the last term represents the rotation energy. The dynamics of the system is governed by the Landau-Lifshitz (LL) equations which in the rotating frame of reference have the form

$$\frac{\delta\mathcal{S}}{\delta m_z}-\frac{\eta}{1-m_z^2}\frac{\delta\tilde{\mathcal{E}}}{\delta\tilde{\phi}}=0,\quad \frac{\delta\mathcal{S}}{\delta\tilde{\phi}}+\eta(1-m_z^2)\frac{\delta\tilde{\mathcal{E}}}{\delta m_z}=0,$$

where $\mathcal{S}=\int d\tilde{t}d\boldsymbol{r}(1-m_z)\partial_{\tilde{t}}\tilde{\phi}-\tilde{\mathcal{E}}$ and η being the LL damping constant.

Since in the rotating frame of reference the energy is time independent, the dip can be considered as a stationary state of the system. To gain some insight to the dip creation we expand the out-of-plane component m_z and the phase ϕ in terms of the magnon eigenfunctions $(\mu_m(r,\chi),\psi_m(r,\chi))\equiv(f_{|m|}(r),g_{|m|}(r))e^{im\chi}$ with the eigenfrequencies $\omega_{|m|}$ on the planar vortex background[14]

$$m_z=\sum_m \alpha_m(t)\mu_m(r,\chi),$$

$$\phi=\chi+\mathfrak{C}\frac{\pi}{2}+\sum_m \beta_m(t)\psi_m(r,\chi), \tag{1}$$

where $\alpha_m=\alpha_{-m}^*$ and $\beta_m=\beta_{-m}^*$ are time dependent coefficients. Inserting expansion (1) into the LL equations and using the orthogonality of the functions (μ_m,ψ_n) we obtain equations for the coefficients α_m and β_m, carrying out integrations over the spatial coordinates. The resulting equations are quite cumbersome, and we will not reproduce them here. Instead, we will consider only the first three modes $m=0,\pm1$ and take into account only cubic nonlinear terms in magnetic energy $\mathcal{E}$,

$$\dot{\alpha}_0=-\omega_0\beta_0-\eta\omega_0A_0\alpha_0,$$

$$\dot{\alpha}_1=-\omega_1\beta_1+i\alpha_1(2k\alpha_0+\omega)-\mathfrak{C}b_e-\eta\omega_1A_1\alpha_1,$$

$$\dot{\beta}_0=\omega_0\alpha_0+2ik(\alpha_1\beta_1^*-\alpha_1^*\beta_1)-\eta\omega_0B_0\beta_0,$$

$$\dot{\beta}_1=\omega_1\alpha_1-i\beta_1(2k\alpha_0-\omega)-\eta\omega_1B_1\beta_1, \tag{2}$$

where $A_m=\langle g_m^2\rangle$, $B_m=\langle f_m^2\rangle$, the coefficient $k=\ell^2\langle f_0f_1g_1/r^2\rangle$ is due to the nonlinearity, $b_e=\frac{b}{2}\langle g_1\rangle$ is an effective strength of the magnetic field, and it is assumed that $\eta\ll1$. Here the notation $\langle\xi\rangle=\int_0^R r\xi dr$ is used. Thus the problem under consideration is reduced to the set of three nonlinearly coupled oscillators. The stationary state of these equations is identified as a dip and the stationary amplitude $\bar{\alpha}_0$ characterizes the asymmetry of the dip profile. In the no-damping ($\eta=0$) and weakly nonlinear ($|k\alpha_0|\ll1$) limit the stationary values $\bar{\alpha}_m$

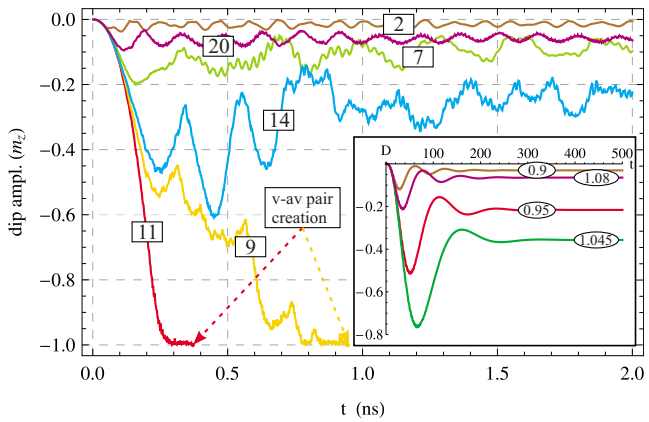

FIG. 4. (Color online) Amplitude of $m_z(t)$ at the minimum (dip center) for the disk ($2R=150$ nm, $h=15$ nm) under the influence of rotating field with a fixed amplitude $B=20$ mT and different frequencies. Numbers in rectangular frames denote frequencies in GHz. The inset contains the time dependence of the dip size parameter, D (see text), obtained from the effective Eq. (2) for $\omega_0=1.5$, $\omega_1=1$, $b_e=0.1$, $\eta=0.02$, $k=0.1$, and $A_{0,1}=B_{0,1}=1$. Corresponding frequencies in dimensionless units are shown in oval frames.

can be presented approximately as $\bar{\alpha}_0 \approx -4k\omega\omega_1 b_e^2/[\omega_0(\omega^2 - \omega_1^2)^2]$, $\bar{\alpha}_1 \approx i\mathcal{C}b_e\omega/(\omega_1^2 - \omega^2)$.

To identify and quantitatively describe the asymmetry of the dip structure we use the parameter: $D = |\int re^{i\chi} m_z^2 d\boldsymbol{r}| \sim \alpha_0|\alpha_1|$, which demonstrates the narrow resonance behavior about ω_1, see inset in Fig. 4. As a result of rotation, the magnon frequencies in the rotating frame of reference are shifted, $\tilde{\omega}_m = \omega_m - m\omega$, and the dipole magnon mode (i.e., the azimuthal mode with $m=1$ for $\omega > 0$ and $m=-1$ for $\omega < 0$) becomes soft, which can be identified from Fig. 3. Near the resonance where $\tilde{\omega}_1$ is small, the nonlinear terms in Eq. (2) become crucial and the system goes to a new regime with a finite value of D (see the inset in Fig. 4). We identify the appearance of a finite D with the dip creation. The dip direction is determined by the product ω: when $\omega > 0$ (< 0) the out-of-plane component of magnetization is negative (positive). This result is in full agreement with the results of full-scale numerical simulations.

In conclusion, we showed that in the presence of *immobile* planar vortex the rotating magnetic field produces a vortex-antivortex pair. This process is the most efficient in a finite frequency interval which is determined by the aspect ratio and material properties of the nanoparticle. The physical reason of the dip creation with a consequent vortex-antivortex nucleation is softening the dipole magnon mode and magnetic field induced breaking cylindrical symmetry in the rotating frame of reference. In some respects such softness of modes due to rotation is similar to the problem of instability of BEC under rotation,[15] and to the Zel'dovich-Starobinsky effect for a rotating black hole.[16] Under the continuous pumping, the soft mode is excited, and the system goes to the nonlinear regime, which results in the dip formation.

The authors thank H. Stoll and B. Van Waeyenberge for helpful discussions. The authors thank the MPI Stuttgart, where part of this work was performed, for kind hospitality and acknowledge the support from Deutsches Zentrum für Luft- und Raumfart e.V., Internationales Büro des BMBF in the frame of a bilateral scientific cooperation between the Ukraine and Germany, Project No. UKR 08/001.

*Corresponding author. vkravchuk@bitp.kiev.ua

[1] R. P. Cowburn, J. Magn. Magn. Mater. **242-245**, 505 (2002).
[2] B. Van Waeyenberge *et al.*, Nature (London) **444**, 461 (2006).
[3] K.-S. Lee, S.-K. Kim, Y.-S. Yu, Y.-S. Choi, K. Y. Guslienko, H. Jung, and P. Fischer, Phys. Rev. Lett. **101**, 267206 (2008).
[4] A. Vansteenkiste *et al.*, Nat. Phys. **5**, 332 (2009).
[5] V. P. Kravchuk, D. D. Sheka, Y. Gaididei, and F. G. Mertens, J. Appl. Phys. **102**, 043908 (2007).
[6] B. A. Ivanov and C. E. Zaspel, Phys. Rev. Lett. **94**, 027205 (2005).
[7] C. E. Zaspel, B. A. Ivanov, J. P. Park, and P. A. Crowell, Phys. Rev. B **72**, 024427 (2005).
[8] R. Zivieri and F. Nizzoli, Phys. Rev. B **78**, 064418 (2008).
[9] We used for all OOMMF simulations material parameters adopted for the Py particle: the exchange constant $A = 2.6 \times 10^{-6}$ erg/cm, the saturation magnetization $M_S = 8.6 \times 10^2$ G, the damping coefficient $\eta = 0.006$, and the anisotropy was neglected. This corresponds to the exchange length $\ell = \sqrt{A/4\pi M_S^2} \approx 5.3$ nm. The mesh cells have sizes $3 \times 3 \times h$ nm, where h is the thickness of the sample. The applied field was used in form $\boldsymbol{b}(t) = b(1 - e^{-t^2/\Delta t^2})(\cos \omega t, \sin \omega t, 0)$, with $\Delta t = 50$ ps.
[10] R. Hertel and C. M. Schneider, Phys. Rev. Lett. **97**, 177202 (2006).
[11] R. Hertel, S. Gliga, C. M. Schneider, and M. Fähnle, Phys. Rev. Lett. **98**, 117201 (2007).
[12] Y. B. Gaididei, V. P. Kravchuk, D. D. Sheka, and F. G. Mertens, Low Temp. Phys. **34**, 528 (2008).
[13] The cells with fixed magnetization contribute to the effective field but they are omitted from the procedure of numerical time integration of the LL equation.
[14] For the planar vortex the magnon modes with opposite m are degenerated; for the general case see, e.g., Ref. 17.
[15] T. Isoshima and K. Machida, Phys. Rev. A **60**, 3313 (1999).
[16] H. Takeuchi, M. Tsubota, and G. Volovik, J. Low Temp. Phys. **150**, 624 (2008).
[17] B. A. Ivanov and C. E. Zaspel, Appl. Phys. Lett. **81**, 1261 (2002).